346 | August 1976

SCHRIFTENREIHE SCHIFFBAU

W.C. Webster

The Computation of the Hydrodynamic Forces Induced by General Vibration of Cylinders

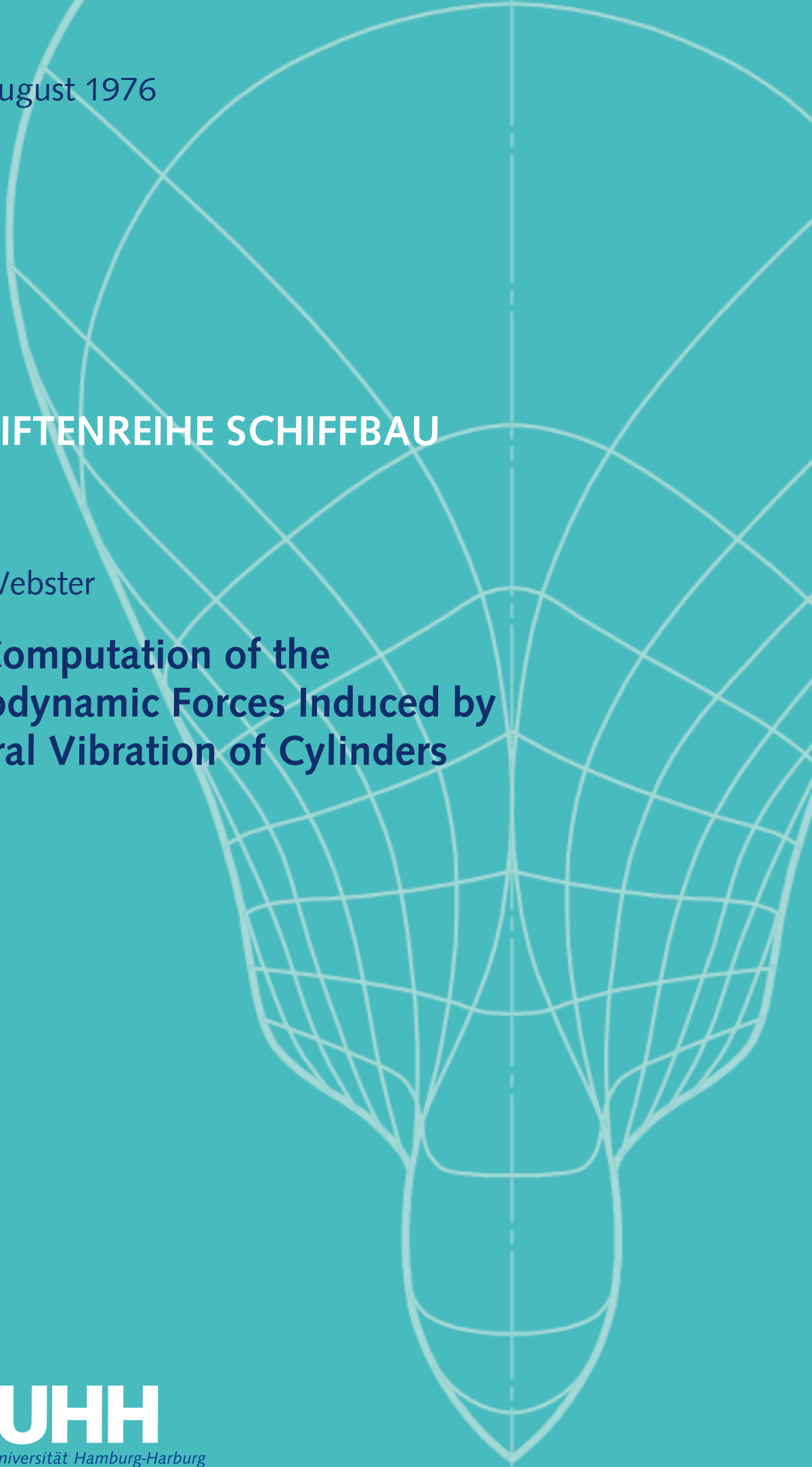

TUHH
Technische Universität Hamburg-Harburg

The Computation of the Hydrodynamic Forces Induced by General Vibration of Cylinders

W.C. Webster

Hamburg, Technische Universität Hamburg-Harburg, 1976

Schriftenreihe Schiffbau
Schwarzenbergstraße 95c
D-21073 Hamburg

http://www.tuhh.de/vss

INSTITUT FÜR SCHIFFBAU
DER UNIVERSITÄT HAMBURG

The Computation of the Hydrodynamic Forces Induced by General Vibration of Cylinders

W.C. Webster

August 1976

Bericht Nr. 346

The Computation of the Hydrodynamic Forces Induced by General Vibration of Cylinders

by

William C. Webster [+)]

+) Associate Professor, The University of California, Berkeley, and currently an Alexander von Humboldt-Stipendiat at the Institut für Schiffbau, Hamburg, and in cooperation with the Sonderforschungsbereich 98.

Introduction

"Ship vibrations" is a title used by various authors to describe not a single phenomena, but rather a broad collection of loosely related topics. These topics can be categorized by the frequency of vibration, since the individual phenomena lead to somewhat disjoint frequency ranges, as can be seen qualitatively in Figure 1.

At extremely low frequencies, the ship vibrates as a rigid or near rigid body under excitation by the wind, waves or even by steering. At somewhat higher frequencies, one observes the beam-like motions of the ship. On these vibrations the ship bends or twists, but the sections do not deform. Generally, these vibrations are excited by the action of propulsion and by slamming. At the very high frequency end we have local vibrations. A typical situation for this would be a machine, which perhaps due to some internal unbalance, vibrates on its mount or supporting structure. These latter vibrations are of sufficiently high frequency and sufficiently localized that the external hydrodynamics does not seem to play a major role. In the above two low frequency cases the external hydrodynamics, including all of the complexities of wave generation due to the vibrations appears to be of great importance.

The area of principal interest here is the somewhat gray area between the low frequency and high frequency vibration problems, a region which can be typified as one in which deformation of the ship cross-sections plays an important role. The appearance of substantial deformation of the ship sections occurs first in the higher longitudinal bending modes (Meijers, 1974, shows a substantial deformation already in the fifth bending mode). At these lower

bending modes the section deformation appears to change slowly in the length direction and one could suppose that the external hydrodynamics of the ship could be treated by using a strip method. At higher frequencies the characteristic length of deformations in both the length and girth directions become comparable and it is clear that any handling of the external hydrodynamics must address the full, three-dimensional character of the vibration pattern.

The calculation of such a vibrational response of a ship requires the treatment of the structure of the ship (in order to determine the internal forces created by deformations) as well as the fluid outside the ship (in order to determine the corresponding hydrodynamic forces). Progress towards determining the hydrodynamic effects in this vibration region has been made principally by Grim (1960 and 1975). However, these results apply to special shapes (flat plates and circular cylinders) and to prescribed deformation patterns. The aim of this paper is to develop a procedure for prediction of the hydrodynamic forces which does not have these limitations and, specifically, a procedure which is well suited for use with modern methods of structural analysis.

In the last two decades powerful, finite element methods have been developed which are now frequently used to characterize the response of complicated structures. (for instance, see Paulling 1963 or Zienkiewicz 1971). It is not to the point here to reiterate this process of analysis in detail, but it is worthwhile to present a skeleton of this analysis in order that the motivation of this present research be clearly seen.

Let us assume that the pertinent part of the ship's structure is decomposed into a series of adjoining, simple structural elements (usually flat plates or straight bars). The displacements of the corners of these elements, and sometimes of other boundary or internal points, are used to describe the deformation of the whole structure. If we let $\mathbf{v}$ be a vector, the components of which are the totality of these nodal displacements, then the usual structural finite element analysis yields in the end a relation

$$\mathbf{K}\mathbf{v} = \mathbf{f} \quad +) \tag{1}$$

where $\mathbf{K}$ is the so-called stiffness matrix and $\mathbf{f}$ is a vector of forces at the corresponding modes.

If the ship is undergoing periodic vibration, then we may express

$$\mathbf{v} = \mathrm{Re}\left\{\mathbf{v}_o e^{-i\omega t}\right\} \tag{2}$$

where $\mathbf{v}_o$ is a vector of complex displacement amplitudes. Corresponding to this motion, there will be internal inertial forces created by the masses of the individual pieces of ship structure, machinery and cargo, and there will be external hydrodynamic forces. The equation of motion for such a problem is

$$(\mathbf{K} - \omega^2\mathbf{M})\mathbf{v}_o = \mathbf{r}_o + \mathbf{f}_{eo} \tag{3}$$

+) we will adopt the convention here of using capital letters for matrices and lower case ones for vectors.

where

$\mathbf{r} = \mathbf{r}_o e^{-i\omega t}$ is the vector of external hydrodynamic forces (referred to the modes)

$\mathbf{M}$ = is the finite-element mass matrix

$\mathbf{f}_e = \mathbf{f}_{eo} e^{-i\omega t}$ is the vector of external exciting forces (referred to the nodes).

It should be noted that the components of $\mathbf{K}$ and $\mathbf{M}$ are real, but those of $\mathbf{r}_o$ and $\mathbf{f}_{eo}$, and thus those of $\mathbf{V}_o$ may not be.

We are generally interested in two different solutions of (3). The first and most common is the determination of the natural modes and resonant frequencies. These are deformations which are sustained by little or no external forces (resonance). They are determined as the solution of (3) with $\mathbf{f}_{eo} \equiv 0$. From a practical point of view the resonant frequencies are most important, since one would like to design the ship and machinery to avoid excitation of the corresponding resonant modes. Another type of analysis, but not as often performed, is the determination of the deformation pattern, $\mathbf{V}_o$, created by a known excitating pattern $\mathbf{f}_{eo}$. It is clear that in order to solve either of these problems we must determine the hydrodynamic forces, $\mathbf{r}_o$. These cause a problem since they are created by the very motion that we wish to determine. It will turn out that if we presume that the motion is small, so that the problem can be linearized, then we can express $\mathbf{r}_o$ in terms of $\mathbf{V}_o$ in a simple fashion, given by

$$\mathbf{r}_o = \omega^2 \mathbf{H} \mathbf{V}_o \qquad (4)$$

The matrix, $\mathbf{H}$, is an array of hydrodynamic influence coefficients each of which represents the force created at one node due to the motion at another. On the subsequent development, it will also turn out that for very high frequencies $\mathbf{H}$ is real and independent of ω. However, at lower frequencies $\mathbf{H}$ becomes complex and dependent on ω. This arises due to the creation of waves, a frequency dependent process. The complex nature of $\mathbf{H}$ at the lower frequency implies that the created waves drain energy from the vibrating structure and thus gives rise to an effective damping of the motion.

For the case of forced motions, the use of $\mathbf{H}$ in (4) leads to a solution

$$\mathbf{v}_o = \left\{\mathbf{K} - \omega^2 [\mathbf{M} + \mathbf{H}]\right\}^{-1} \mathbf{f}_{eo} \tag{5}$$

where the symbol $\{\cdot\}^{-1}$ implies the inverse matrix. For the case of natural modes, we seek a solution for $\mathbf{f}_{eo} \equiv 0$, or

$$\left\{[\mathbf{M} + \mathbf{H}]^{-1} \mathbf{K}\right\} \mathbf{v}_o = \omega^2 \mathbf{v}_o \tag{6}$$

This is clearly an eigenvalue problem, where the eigenvalues themselves correspond to the square of the resonant frequencies, and the eigenvectors to the natural modes. It should be noted that at low frequencies H is complex and, a solution to the eigenvalue problem may not exist. If the imaginary part of $\mathbf{H}$ is relatively small (that is, the hydrodynamic damping is relatively small), then a good estimate of the mode shapes and resonant frequencies can be found by replacing $\mathbf{H}$ by $\mathrm{Re}(\mathbf{H})$ in (6).

On conclusion, the analysis of vibration of ships can be directly performed using the already well developed finite-element structural analysis procedures if one can find a representation of the hydrodynamic forces in the form of (4). That is, as the product of a matrix $\mathbf{H}$, which is dependent on the ship geometry, but not its vibrational motions distribution, and of a vector $\mathbf{V}_o$ which only depends on the motion. The remaining sections of this paper are devoted to this task.

Two Dimensional Deformations

For the lower frequency vibrations, say, for instance, the fourth or fifth beam-like modes, the individual sections may undergo significant deformation together with a general translation or rotation. If the section shape and also the motion distribution change slowly in the lengthwise direction, then it may be appropriate to use a strip theory, as described by Klein, 1967. The three dimensional hydrodynamics are approximated by the use of two-dimensional flows about the cross-sections.

Consider the oscillation of the skin of a two-dimensional section shown in Figure 2. The deformation pattern, $A_2(s,t)$ is specified as a motion measured along the normal to the undisturbed section. Tangential deformations are ignored since their effect would only be local through the action of viscosity in the water. We will assume that the deformation is sinusoidal and is given by

$$A_2(s,t) = \mathcal{R}e\left\{a(s)\, e^{-i\omega t}\right\} \qquad (7)$$

where $a(s)$ is a complex function of s . We will also make the following assumptions:

i) The fluid is incompressible and inviscid, and the flow is irrotational. Effects such as surface tension, cavitation etc. are ignored also. As a result, the fluid motion can be described by a potential, $\varphi(x,y;t)$, which satisfies LaPlace's equation $\Delta\varphi = 0$ in the fluid domain.

ii) The motions are small enough so that the nonlinear boundary conditions on the body and free surface may be replaced by linear boundary conditions on the mean section and the undisturbed free surface, $z=0$. On the body this boundary condition is $\varphi_n = A_t(s,t)$ and on the free surface the appropriate condition is $\varphi_{tt} + g\varphi_z = 0$

A solution, φ, to this boundary value problem can be obtained as a distribution of oscillatory source Green functions, $G(y,z;\eta,\zeta;t)$ on the periphery of the submerged contour C_o, as given by

$$\varphi(y,z;t) = Re\left\{\int_{C_o} Q(s')\, G(y,z;\eta(s'),\zeta(s');\omega)\, e^{-i\omega t}\, ds'\right\} \tag{8}$$

The Green Function, G, is source like when (y,z) approaches (η,ζ) and satisfies the free surface boundary condition given in ii) above. This Green function is well known and given, for instance, by Wehausen as

$$G(y,z;\eta,\zeta;\omega) = \frac{1}{2\pi} Re\left\{\begin{array}{l} \ln\beta_1 - \ln\beta_2 \\ +2\,p.v.\int_0^\infty dk\, e^{-ik\beta_2}/(\nu-k) \end{array}\right\} \tag{9}$$
$$-i\, Re\left\{e^{-i\nu\beta_2}\right\}$$

where

$$\beta_1 = (y-\eta) + i(z-\zeta),$$
$$\beta_2 = (y-\eta + i(z+\zeta),$$
$$\nu = \omega^2/g.$$

The first two terms in (9), the logarithmic terms, represent the flow created by a source in the fluid and a sink at the so-called "mirror image" point. These terms are not dependent on the frequency of oscillation, ω. The remaining terms, however, are and are associated with the creation of waves on the water surface. At high frequencies, these terms become very small and can be ignored or, as shown in a later section, simplified.

The function $Q(s')$ in (8) is the complex strength of the oscillating source distribution and must be chosen so that the kinematic boundary condition on the body, ii) above, is satisfied. As a result, we have the following complex equation

$$\left\{ (\mathbf{N}\cdot\nabla) \int_{C_o} Q(s')\, G\, ds' \right\}\Big|_{C_o} = -i\omega\, a(s) \quad +) \tag{10}$$

where $\mathbf{N}$ is the outward unit normal and ∇ is the gradient operator .

The appropriate, linearized form of the pressure equation is $p(s,t) = -\rho\, \Phi_t$, or

$$p(s,t) = \rho\, \mathrm{Re} \left\{ i\omega\, e^{-i\omega t} \int_{C_o} Q(s')\, G\, ds' \right\} \tag{11}$$

---

*) For simplicity, we adopt the convention here and throughout the rest of the paper that the arguments of G and other functions will be enumerated only when needed for clarity.

Before we start with the solution of (10), it is instructive to first consider a special selection of $\alpha(s) = \delta(\tilde{s}-s)$, a Dirac Delta function. The solution source density obtained from (10) is both a function of s and of the parameter $\tilde{s}$. We will denote this solution by $\tilde{Q}(s,\tilde{s})$ and presume, for the moment, that this function is known. Thus

$$\left\{ (\mathbf{N}\cdot\nabla) \int_{C_o} \tilde{Q}(s',\tilde{s})\, G\, ds' \right\}\Big|_{\epsilon_o} = -i\omega\,\delta(\tilde{s}-s) \qquad (12)$$

If we multiply both sides of (12) by an arbitrary deformation distribution $\alpha(s)$ and integrate with respect to $\tilde{s}$, we get, after rearrangement

$$\left\{ (\mathbf{N}\cdot\nabla) \int_{C_o} \left[\int_{C_o} \alpha(\tilde{s})\, \tilde{Q}(s',\tilde{s})\, d\tilde{s} \right] G\, ds' \right\}\Big|_{C_o} = -i\omega\,\alpha(s) \qquad (13)$$

The term in the [ ] brackets of (13) is, by comparison with (10), the required source density for the flow created by the deformation $\alpha(s)$. Inserting this source density in (11) and again rearranging, we obtain

$$p(s,t) = \mathrm{Re}\left\{ e^{-i\omega t} \int_{C_o} \alpha(\tilde{s})\, T(s,\tilde{s})\, d\tilde{s} \right\} \qquad (14)$$

where

$$T(s,\tilde{s}) = i\rho\omega \int_{C_o} \tilde{Q}(s',\tilde{s})\, G\, ds'$$

It is clear that $T(s,\tilde{s})$ is a function <u>independent</u> of the deformation pattern, $\alpha(s)$, although it is dependent on the section contour C_o. As such $T(s,\tilde{s})$ captures the essential hydrodynamics of the flow about this section. It is the pressure at a point s due to a unit motion at $\tilde{s}$ and is precisely the type of influence function we need in order to generate an influence matrix $\mathbf{H}$ given in (4).

A few other choices of $a(s)$ are worth mentioning. If $a(s) = n_y$, the y component of the unit normal, then the resulting deformation corresponds to pure sway. Similarly $a(s) = n_z$ results in pure heave. In other words, special choices of $a(s)$ lead to flows about rigid sections, and these flows have been treated by many researchers. There appears to be no closed-form solution to these rigid body flows for sections of arbitrary shape and, therefore, it seems unlikely that a closed-form solution for $Q(s,\tilde{s})$ introduced above will be forthcoming. Among the approximate methods, the "close-fit" method of Frank, 1967 appears to be best suited for extension to the arbitrary deformation vibration problem since it is already a finite element approach. We will therefore adopt this approach here as a foundation and use the general solution method using δ functions described above as a model for this extension.

The "Close-Fit"-Method for Arbitrary Deformations

In this development a somewhat different and, it is believed, more consistent philosophy is used than in the original paper by Frank. Here, we will avoid the apparent solving the integral equation (10) only at a fixed number of points. Rather we will maintain the functional character of both right and left-hand sides of (10). In the end our formulation results in the same one which one would get if the Frank approach were carried forth consistently. However, it is believed that the approach presented here displays perhaps a bit better the level of approximation which is assumed.

We will approximate the given contour by n straight line segments as shown in Figure 3. The coordinates S_1 (on the undisturbed free surface on the right) and S_2 are the end points of the first segment; S_n and S_{n+1} (on the undisturbed free surface on the left) are the end points for the n th segment. Frank's procedure for discretization is that along this new polygonal contour, C, we will approximate all functions piecewise by segments of constant value. This latter value is chosen to be the value of the function at the center of the corresponding line segment. For this purpose, we define

$$\left.\begin{aligned} f_i(S) &= 1 \\ &= 0 \end{aligned}\right\} \text{if} \quad \begin{aligned} &S_i \leqslant S < S_{i+1}, \\ &\text{otherwise} \end{aligned} \tag{15}$$

$$\bar{S}_i = \tfrac{1}{2}(S_i + S_{i+1})$$

$$\bar{y}_i = \tfrac{1}{2}(y_i + y_{i+1})$$

$$\bar{z}_i = \tfrac{1}{2}(z_i + z_{i+1})$$

The function $f(S)$ here plays a role which can be characterized as a finite-element delta function.

Using these definitions, we make the following finite element approximations

$$a(S) \approx \sum_{i=1}^{m} a(\bar{S}_i) f_i(S) = a_i f_i(S) \quad +)$$

$$Q(S) \approx \sum_{i=1}^{m} a(\bar{S}_i) \tilde{Q}(S,\bar{S}_i) \quad \text{and} \quad (16)$$

$$\tilde{Q}(S,\bar{S}_i) \approx \sum_{j=1}^{m} q(\bar{S}_j,\bar{S}_i) f_j(S) = q_{ij} f_j(S)$$

The motivation for the second expansion in (16) stems directly from and by analogy to (13). At this point it is yet to be proved that such an expansion is appropriate. Also, for clarity, we will use index notation rather than vector notation here. Inserting (16) into (10) we get

$$a_i q_{ij} \left\{ (\mathbf{N}\cdot\nabla) \int_c f_j(S') G \, dS' \right\}\Big|_c = -i\omega a_i f_i(S) \quad (17)$$

If we let

$$\left\{ (\mathbf{N}\cdot\nabla) \int_c f_j(S') G \, dS' \right\}\Big|_c = B_j(S)$$

and

$$B_j(S) = \sum_{k=1}^{m} B_j(\bar{S}_k) f_k(S) = b_{jk} f_k(S) \quad (18)$$

then (17) becomes

+) As a shorthand, we use the standard convention that when indicies are repreated, summation is implied.

$$a_i\, q_{ij}\, b_{jk}\, f_k(s) = -i\omega a_i\, f_i(s) \qquad (19)$$

Since the "f" functions are orthogonal over the submerged contour (for any given value of s, only one function f_i, $i = 1, m$ is different from zero), then we may equate the right hand side termwise to the left, or

$$a_i\, q_{ij}\, b_{jk} = -i\omega a_k\,, \quad k = 1, m \qquad (20)$$

It can be seen by inspection that the choice $q_{ij} = -i\omega\, b^{-1}_{ij}$ transforms (20) into an identity, where b^{-1}_{ij} is the inverse of b_{jk} (i.e. $b^{-1}_{ij}\, b_{jk} = 1$ if $i = k$, and 0 otherwise). That is, this choice of q_{ij} solves the flow problem <u>independent</u> of the particular choice of deformation pattern a_k.
The corresponding source strength is then

$$Q(s) = -i\omega\, a_i\, b^{-1}_{ij}\, f_j(s) \qquad (21)$$

If we insert this source strength into the pressure integral, (11), we get

$$p(s,t) = \rho\, \mathrm{Re}\left\{\omega^2 a_i\, b^{-1}_{ij}\, e^{-i\omega t} \int_c f_j(s')\, G\, ds'\right\} \qquad (22)$$

If we let

$$\left\{ \int_c \phi_j(S')\, G\, dS' \right\}\Big|_c = U_j(S) \quad \text{and}$$

$$U_j(S) \approx \sum_{k=1}^{m} U_j(\bar{S}_k)\, \phi_k(S) = u_{jk}\, \phi_k(S) \qquad (23)$$

then we may rewrite (22) as

$$p(S,t) = \mathrm{Re}\left\{ \rho \omega^2\, a_i\, b_{ij}^{-1}\, u_{jk}\, \phi_k(S) \right\} \qquad (24)$$

If we are interested in $r_k = \mathrm{Re}\{ r_{ko}\, e^{-i\omega t} \}$, the oscillating normal force on any segment k (of unit width), then we must multiply this pressure by the length of this segment, d_k. Thus,

$$r_{ko} = \omega^2\, a_i\, h_{ik} \qquad (25)$$

where

$$h_{ik} = \rho\, b_{ij}^{-1}\, u_{jk}\, d_k$$

Equation (25) is then the formula for the required influence matrix, $\mathbf{H}$, shown in (4).

Formulas for the matrix components b_{ij} and u_{jk} using the Green function (9) are given by Frank. In order to use (25) we need only find the inverse of b_{ij}

Two-Dimensional Results

a. High Frequency

Using the procedures presented by Frank and the pressure influence function, $b_{ij}^{-1} u_{jk} f_k(s)$, shown in (24) was computed for a variety of cases. This first set of cases corresponds to the case of $\omega \to \infty$ whereby the wave dependent parts of (9) vanish, leaving only the two logarithmic terms. For most of the vibration problems for which a general deformation pattern is important, this assumption is quite accurate. A further investigation of this point will be made below.

Three section shapes were investigated: a half circle, a rectangle and a triangle. All three were decomposed into 24 segments. The computed pressure influence functions are shown in Figures 4-6. These functions give the non-dimensional pressure per unit width generated around the section due to the motion of the i^{th} segment. One can see that these motions lead to pressure distributions which are maximum at the moved segment and somewhat slowly decay, approaching zero at the free surface. As a result these pressure functions are not symmetric with respect to the centerline, although the sections are. Further, one can see that motions of the segments near the free surface produce much smaller pressure changes (both on the moved segment and elsewhere) than the same motion at a deeply submerged segment. This result is new only in this context, since this fact has been known for years by hydroacousticians.

As a check of the accuracy of the procedure, computations were made of the rigid body added masses in sway and heave by taking $a(s)$ equal to n_y and n_z respectively. These values were compared with exact computations for these sections and errors in the order of 3 % were obtained. An increase in the number of segments from 24 to 40 reduced the error to less than 1 %.

Figure 7 shows four different deformation patterns assumed for the rectangular cross-section and the corresponding computed pressure distribution. The first pattern is that in which $a(s)$ is constant. This corresponds to a breathing motion where the whole section grows and shrinks periodically. The second deformation pattern has $a(s)$ constant on the bottom and zero on the sides. This corresponds to pure heaving. The last two deformation patterns might be due to typical vibrations. The first of these is symmetric about the centerline and the second is neither symmetric nor asymmetric. All of these deformation patterns have the same motion at segment 12 (next to the centerline on the bottom). One can readily see that the pressure which occurs at this point is strongly dependent on the shape of the deformation pattern. The reason for this behavior is clear. The pressure influence functions are rather broad functions, in the sense that motion at one segment creates substantial pressures in the whole neighbourhood of the segment. When we have a deformation pattern in which the section expands ($a(s) > 0$), in one region and contracts ($a(s) < 0$) in the neighboring region, then the induced pressures tend to cancel one another. This observation explains the results of Grim, 1975, where he shows that the flow about an oscillating circular cylinder produces smaller pressures when the wave length of the deformation pattern around the periphery becomes small.

We see then that the usual assumption of a fixed, hydrodynamic mass per segment (c.f. Grim 1975) must be considered only a crude approximation for use in performing engineering calculations. Further, in any case, the induced pressures, and thus the effective added masses in the neighbourhood of the free surface are much smaller than those near the ship bottom. The decrease in induced pressures with decreasing girth wave length reported by Grim and also determined here gives a theoretical justification for ignoring hydrodynamic effects for the case of high frequency, local vibrations.

b. Moderate Frequency

The procedure for the computation of the oscillatory flow about an arbitrary section using the full Green function given in (9) is worked out by Frank and could, in principle, be carried over here. However, as pointed out by Frank in this context (and by Fritz-John, 1950 for the general case) this solution procedure breaks down at infinitely many special frequencies. These frequencies are associated with slashing modes internal to the body. Because of round-off errors and other inaccuracies the computation becomes ill-conditioned even in the neighborhood of these critical frequencies. For the most part the lowest critical frequency is already in the upper range of interest for ship motions and its existence does not cause many problems in the computation of the corresponding, rigid-body flows. However, in the frequency range that we are interested in these critical frequencies occur quite frequently and do cause problems.

A procedure for avoiding this problem is available for these higher frequencies. First, let us make an asymptotic expansion of the principal value integral in (9) appropriate for large values of $\nu|\beta_2|$ where $\beta_2 = (y-\eta)+i(z+\zeta)$ as before. As $\nu|\beta_2| \to \infty$, we have

$$\text{p.v.}\int_0^\infty dk\,\frac{e^{-ik\beta_2}}{\nu-k} \approx i\pi e^{-i\nu\beta_2} + \sum_{m=1}^{'}(m-1)!\,(-i\nu\beta_2)^{-m} \qquad (26)$$

The summation shown in (26) is asymptotic in nature and does not converge. For large values of $\nu|\beta_2|$, the first few terms give a good approximation. Inserting the above expression into (9), we obtain

$$\bar{G}(y,z;\eta,\zeta;\omega) = \frac{1}{2\pi}\,\mathrm{Re}\left\{\begin{array}{l}\ln\beta_1 - \ln\beta_2 \\ +2\sum_{m=1}^{'}(m-1)(-i\nu\beta_2)^{-m}\end{array}\right\} \qquad (27)$$

$$-i\,e^{-i\nu\beta_2'},$$

$$\beta_2' = -(y-\eta)+i(z+\zeta)$$

This approximate Green function can be easily interpreted. The first term includes the source singularity, $\ln\beta_1$, and other terms involving β_2 which are smooth (that is, not wavy) functions of β_2. The lastterm contains all of the character of the free surface waves. This last term is bounded in magnitude by $\exp[\nu(z+\zeta)]$; and on the bottom of a ship of draft T, this bound is $\exp[-\nu T]$. For a typical case under consideration here (νT) is at least 20 and more usually 100. As a result, the value of the lastterm in (27) for a location on the bottom of the ship is less than 10^{-9} for our range of interest. This is only another way of stating that at high frequencies the wave length is short and that the fluid motion created by these waves remains in a thin layer extending about one wave length below the free surface.

We may use these observations in the following way. Wave motion created on one side of the ship can affect the flow on the other side of the ship only by inducing a flow underneath the ship, since there is no other path of communication between the sides. The above remarks show that if the frequency of the created waves is relatively high, no flow is induced underneath the ship and thus the wave motion on one side of the ship is sensibly independent of that on the other side. The exact Green function (9) and the approximate one (27) do not show this separation since they are derived assuming there is a free-surface along the whole line z=0. That is, the Frank solution procedure implicitly constructs a flow in which there is a flow internal to the ship contour as well as that external. The formal, computed interaction of the waves created by the two ship sides at high frequencies occurs only through the fictitious flow within the section contour, since, as described above it cannot occur through a flow outside the contour.

As a result then, we shall modify our application of the Green function in (27) by setting the last term (that is, the wave term) equal to zero when $\eta y < 0$, i.e. when (y, z) is on the side of the ship opposite to (η, ζ). This separation of the wave effects between the sides of the ship eliminates the critical frequency problems. It should be pointed out that the argument which leads to this separation only applies at high frequency and can not be used, for instance, to eliminate the lowest critical frequency. Further, we can see from the above argument that the creation of waves, that is the generation of external damping for general deformation vibrations, is concentrated in the two regions of the section near the free surface.

Using the Green function given in (27) leads to values of b_{jk} which are complex and, as a result the inverse matrix b^{-1}_{jk} is also complex. The finite element pressure functions are likewise complex and, therefore, so is h_{ik} in (25). Computations for the rectangular cross-section shown in Figure 6 were made including the high frequency free surface effect by using $\bar{G}$ (modified as described above to eliminate the critical frequency problem). The results are shown in Figure 8 for $\frac{\omega^2 B}{2G} = 2 \rightarrow 20$. One can see that only at the topmost segments are there any discernable differences in the real (in-phase) pressures, and these differences are slight. The imaginary (out-of-phase) pressures are all small, but are very dependent on the value $\omega^2 B/2g$. We can conclude that for the purpose of determining the normal mode shapes and natural frequencies, it is probably sufficient to compute only the $\omega \rightarrow \infty$ results previously presented.

As the results above show, the consideration of wave making effects does not greatly modify the real (in-phase) pressures created around a section over those which would occur, if the assumption $\omega \rightarrow \infty$ were made. The imaginary (out-of-phase) pressures do not exist when $\omega \rightarrow \infty$ and so it is problematical to assess whether they are small or large for a given, finite $\frac{\omega^2 B}{2g}$. Because these out-of-phase pressures are directly related to wave creation they reflect an energy dissipation or damping. The damping of the vibration is important principally at a resonance, since the size of the response is limited here only by the damping. It seems fair to say that the hydrodynamic damping is important if it is of comparable magnitude to the intrinsic damping of the structure. The latter is typically less than 5 % of critical damping and often more like 1 %. (c.f. Betts, Bishop and Price, 1976).

The determination of the exact contribution of the hydrodynamic damping to the overall damping of a structure requires a detailed knowledge of both the mass and stiffness distributions within the structure. If a particular mode is determined to be important either by solving (6) using $\mathcal{R}_e(\mathbf{H})$ instead of $\mathbf{H}$ computed at the resonant frequency, ω_r, (or alternatively, and somewhat cruder, using $\mathbf{H}$ computed as $\omega \to \infty$), we can express the non-dimensional hydrodynamic damping (damping divided by critical damping) for this mode as follows:

$$\zeta_h = \frac{-\mathcal{I}m\left\{\int_{C_o} a(s)\, p\, ds\right\}}{2\left[\mathcal{R}_e\left\{\int_C a\, p\, ds\right\} + \iint_\Gamma \omega^2 \hat{a}\, \rho_s(y,z)\, dy\, dz\right]} \tag{28}$$

where Γ is the area enclosed by the curve C_o, and $\hat{a}(y,z)$ is the distribution of motion of the structure within the section. When (y', z') lie on the boundary C_o at a point corresponding to s', then $\hat{a}(y',z') = a(s')$. The numerator is proportional to the work dissipated and the [ ] term in the denominator is proportional to the internal kinetic energy. The first term of the denominator is the contribution due to the external fluid and the second is that due to the internal structure. It seems appropriate here to calculate another damping,

$$\zeta' = \left[\frac{-\mathcal{I}m\left\{\int_{C_o} a p\, ds\right\}}{2\,\mathcal{R}_e\left\{\int_{C_o} a p\, ds\right\}}\right] \tag{29}$$

which represents the damping in this mode if the internal structure were massless. Clearly $\zeta'_h > \zeta_h$ (since all of the integrals in (28) are positive) and we can conclude that if ζ'_h is small compared to the intrinsic structural damping then ζ_h certainly is. Figure 9 shows the variation of ζ'_h with $\left(\frac{\omega^2 B}{2g}\right)$ corresponding to

the results shown in Figure 8. It can be seen that for this deformation pattern if $\frac{\omega^2 B}{2g} > 20$, $\zeta_h' < 0.003$ and must be considered negligible.

For an actual case, solution of (6) yields the whole deformation pattern and evaluation of (18) can be made without reference to ζ_h' .

Three Dimensional Vibrations

In the previous section we considered only two dimensional vibrations. This information can be used presumably in a striptheory in order to compute the pressures over a real ship. In this case, one would require that both the original section shape and the deformation pattern change slowly along the ship's length. Let us now assume that the ship is undergoing a higher frequency vibration for which the deformation pattern varies sinusoidally along the ship's length and for which the wave length of the deformation cannot be considered large. It is reasonable to assume that we can still apply a stripmethod to this problem as long as the ship section shape still meets the slow-varying criterion and if we solve the following three-dimensional problem. Let us assume that we form an infinite cylinder with the ship's cross-section. The deformation pattern will be assumed arbitrary around the girth and sinusoidal along the length, and given by

$$A_3(x,s;t) = a(s)\cos\mu x\cos\omega t \qquad (30)$$

where A_3 is, as before, measured normal to the section contour. When $\mu \equiv o$ we obtain our previous two-dimensional case. A solution to the general boundary value problem can also be represented by a distribution of Green functions on the surface of the cylinder by

$$\varphi(x,y,z;t) = Re\int_{-\infty}^{\infty} d\xi \int_{C_o} Q_3(\xi,s')\, G_3(x,y,z;\xi,\eta,\zeta;\omega)\, ds' \qquad (31)$$

For this high-frequency case, the appropriate Green function is independent of ω and given by

$$G_3(x,y,z;\xi,\eta,\zeta) = \frac{-1}{4\pi}\left\{\begin{array}{l}[(x-\xi)^2+(y-\eta)^2+(z-\zeta)^2]^{-1/2} \\ -[(x-\xi)^2+(y-\eta)^2+(z+\zeta)^2]^{-1/2}\end{array}\right\} \quad (32)$$

Like the high-frequency, two-dimensional case this is a source underwater and a sink outside the flow at the image point above the free surface. The kinematic boundary condition on the cylinder surface is then

$$\left\{(\mathbf{N}\cdot\nabla)\int_{-\infty}^{\infty} d\xi \int_{C_o} Q_3(\xi,s')\,G_3\,ds'\right\}\Big|_{C_o} = -i\omega\cos\mu x\, a(s) \quad (33)$$

Let us try a source distribution $Q_3(\xi,s') = \cos\mu\xi\,\bar{Q}(s')$. The left hand side of (33) becomes

$$(\mathbf{N}\cdot\nabla)\int_{C_o} ds'\,\bar{Q}(s')\int_{-\infty}^{\infty}\cos\mu\xi\,G_3\,d\xi \quad (34)$$

From (32) above, we see that the form of G_3 is such that it is a function of $(\xi-x)$ and not of ξ and x independently. We now introduce a new variable $\bar{\xi} = \xi - x$ and (34) becomes

$$(\mathbf{N}\cdot\nabla)\int_{C_o} ds'\,\bar{Q}(s')\int_{-\infty}^{\infty}[\cos\mu x\cos\mu\bar{\xi} - \sin\mu x\sin\mu\bar{\xi}]\,G_3(\bar{\xi},y,z;0,\eta,\zeta)\,d\bar{\xi} \quad (35)$$

Since $G_3(\bar{\xi}) = G_3(-\bar{\xi})$, the term involving $\sin\mu\bar{\xi}$ drops out and thus (33) becomes

$$\left\{(\mathbf{N}\cdot\nabla)\int_{C_0}\bar{Q}(s')\,\bar{G}_3\,ds'\right\}\Big|_{C_0} = -i\omega\,a(s) \tag{36}$$

where

$$\bar{G}_3 = -\frac{1}{2\pi}\left\{\begin{array}{l}\displaystyle\int_0^\infty d\bar{\xi}\,\cos\mu\bar{\xi}\,/\,[\bar{\xi}^2+(y-\eta)^2+(z-\zeta)^2]^{1/2} \\ \displaystyle -\int_0^\infty d\bar{\xi}\,\cos\mu\bar{\xi}\,/\,[\bar{\xi}^2+(y-\eta)^2+(z+\zeta)^2]^{1/2}\end{array}\right\} \tag{37}$$

In (36) we have made use of the fact that $(\mathbf{N}\cdot\nabla)\cos\mu x$ on the cylinder is $\cos\mu x\,(\mathbf{N}\cdot\nabla)$. $\bar{G}_3$ is made of two terms, each of the form

$$\int_0^\infty d\bar{\xi}\,\cos\mu\bar{\xi}\,/\,[\bar{\xi}^2+|\beta|^2]^{1/2} \tag{38}$$

where $|\beta|$ is the two-dimensional distance between (y,z) and (η,ζ) or $(\eta,-\zeta)$. Introducing a new variable $\gamma = \mu\bar{\xi}$, this integral becomes

$$g(\mu|\beta|) = \int_0^\infty d\gamma\,\cos\gamma\,/\,[\gamma^2+(\mu|\beta|)^2]^{1/2} \tag{39}$$

That is, this integral is a function of only the combination $\mu|\beta|$, and we can write (37) as

$$\bar{G}_3 = -\frac{1}{2\pi}\,[g(\mu|\beta_1|)-g(\mu|\beta_2|)] \tag{40}$$

It should be pointed out here that $\bar{G}_3$ is <u>not</u> a harmonic function. Rather it is the Green function which allows us to solve the three dimensional problem using (34), a formula which is of the same form as (10) for the two-dimensional problem. Grim, 1970, has shown that the three-dimensional solution for this problem satisfies a two-dimensional Poisson equation.

The function $g(\mu|\beta|)$ was determined for a wide range of values for $\mu|\beta|$ by numerical integration using Simpson's rule, and is shown in Figure10. For use as a Green function we require that $g(\mu|\beta|)$ behave as $\ln|\beta|$, $|\beta| \to 0$. Without loss of generatily, then, the function $g(\mu|\beta|)$ which behaves as $\ln(\mu|\beta|)$ in this limit, was reduced by the constant $\ln\mu$. It is clear from Fig.10 that the two dimensional and three dimensional Green function behave monotonically, but the slope of g approaches zero as $\mu|\beta|$ approaches infinity much more quickly than the slope of $\ln|\beta|$.

The determination of $\bar{Q}_3(s)$, the girthwise variation of source strength, is performed using the same finite element method as for $Q(s)$. If we let

$$\begin{aligned} B_{3,i} &= \left\{ (\mathbf{N}\cdot\nabla) \int_c \phi_j(s')\, \bar{G}_3\, ds' \right\} = b_{3,ij}\, \phi_j(s) \\ U_{3,j} &= \left\{ \int_c \phi_j(s')\, \bar{G}_3\, ds' \right\} = u_{3,jk}\, \phi_k(s) \end{aligned} \tag{41}$$

then, the pressure acting on the cylinder, $p_3(x,s,t)$ is given by

$$p_3(x,s,t) = \cos\mu x\, \mathrm{Re}\left\{ \rho\omega^2 e^{-i\omega t} a_i\, \bar{b}^{-1}_{3,ij}\, u_{3,jk}\, \phi_k(s) \right\} \tag{42}$$

Calculations of the pressures was performed for the rectangular section considered previously and the results are shown in Figures 10 and 11. In Fig. 10 the amplitude of the pressure is shown (that is, only the part $\mathcal{R}e\{\}$ in (A2)), as a function of the longitudinal wave length $\lambda/B = 2\pi/\mu B$. It is seen that even for very large values, $\lambda/B = 8$, that the three dimensional effects are very strong and the resulting pressures are much smaller than the corresponding two-dimensional case $\lambda/B = \infty$. Even more dramatic are the results for the special cases of deformations which result in heave and sway. With a value of $\mu B/2 = 0.8$, which corresponds to a longitudinal wave length approximately 4 times the beam, the heave added mass is only 60 % of that for infinite wave length (two-dimensional motion.)

Summary and Conclusions

The above computations show that it is relatively simple to extend the method of Frank to compute the hydrodynamic pressure around an arbitrary section undergoing an arbitrary deformation. For simple two dimensional sections undergoing high frequency ($\omega \to \infty$) vibrations, the computation is straight-forward. For finite, but still relatively high frequencies, Frank's method must be modified to eliminate the critical frequency problem. The approach adopted here is asymptotic, that is, applies only to relatively high frequencies and cannot be extended to low frequencies. It was also shown that the extension to deformation patterns which are periodic along the length of an otherwise arbitrary cylinder can also be easily performed. For this problem one obtains a new, non-harmonic Green function.

Computations for all of these formulations were performed and the following conclusions can be shown:

1. Two dimensional deformations ($\omega \to \infty$)
   a. Pressures developed by the motion of one panel of the section (all other panels remaining fixed) are highest at the moved panel and decay gradually reaching zero at the free surface.
   b. Motions of panels near the free surface result in far smaller induced pressures than those deeply submerged.
   c. The pressures created at one panel are due not only to its motion, but also to the motion of the other panels nearby. As a result, when the deformation pattern has many modes around the periphery, the induced pressures are quite small compared to a simple motion (say heaving) where the motion is all of one sign.

2. Two-Dimensional Motions (ω large but finite)
   The effect of wavemaking exists only on those panels quite near the free surface. The panels near the ship bottom are apparently unaffected. For a realistic deformation pattern of a rectangular cross-section it was found that the damping of this vibration mode caused by wave generation was negligible if $\frac{\omega^2 B}{2g} > 20$.
3. Three-Dimensional Motions
   a. The effect of periodic longitudinal variation of the deformation pattern is to reduce the pressures which would have been generated if there were no longitudinal variation.
   b. With very short longitudinal wave lengths (μ -large) the pressures generated at a panel are proportional mostly to the motion of that panel and are fairly independent of the motions of neighboring panels.

Acknowledgement

The author is deeply indepted to his Betreuer Professor Dr.-Ing. Otto Grim at the Institut für Schiffbau, Hamburg, for his many fruitful suggestions concerning this research. The research presented here is built on the foundation developted by Prof. Grim over the last 20 years. The author is also indebted to the Alexander von Humboldt-Stiftung for their support of this work in the Bundesrepublik Deutschland and also to the Germanischer Lloyd, Hamburg.

Bibliography

Betts, C.V., Bishop, R.E.D. and Price, W.G.,
"A Survey of Internal Hull Damping", The Royal Institution of Naval Architects, 1976.

Frank, W., "Oscillation of Cylinders in or below the Free Surface of Deep Fluids", Naval Ship Research and Development Center Report 2375, October 1967.

Grim, O., "Berechnung der durch Schwingungen eines Schiffskörpers erzeugten hydrodynamischen Kräfte. Jahrbuch der Schiffbautechnischen Ges., Vol.47, 1958.

"A Method for a More Precise Computation of Heaving and Pitching Motions both in Smooth Water and in Waves". Proceeding, Third Symposium on Naval Hydrodynamics, Scheveningen, Netherlands, 1960.

and Kirsch, V.,
"Forces on a Two Dimensional Body Excited by an Oblique Wave"

"Hydrodynamische Masse bei lokalen Schwingungen insbesondere bei Schwingungen im Bereich des Maschinenraums, Schiff + Hafen, Heft 11, 1975.

John, F., "On the Motions of Floating Bodies II" Communications on Pure and Applied Mathematics, Vol. 8, Interscience Publishers, Inc., New York, 1950.

Kline, R.G. and Sellers, M.L.,
"Some Aspects of Ship Stiffness", Transactions, SNAME, 1967.

Meijers, P., "Numerical Hull Vibration Analysis of a Far East Container Ship", Netherlands Ship Research Centre, TNO 195 S, July 1974.

Paulling, J.R. jr., "The Analysis of Complex Ship Structures by the Finite Element Technique", Journal of Ship Research, Dec. 1964.

Wehausen, J.V. and Laitone, E.V., "Surface Waves", Handbuch der Physik, edited by S. Flügge, Vol. 9, Fluid Dynamics 3, Springer Verlag, Berlin, Germany.

Zienkiewicz, O.C., The Finite Element Method in Engineering Science, 1971, MacGraw-Hill, New York.

Appendix

In order to compute the pressures induced on a two-dimensional section by an arbitrary deformation pattern we see from (25) that we need the influence elements b_{ij} and u_{jk} . Computation of these elements is given in detail by Frank and only the principal results are tabulated here. Consider a complex function $\gamma(y,z;\eta,\zeta)$ which is analytic in the complex variable $\hat{z}=y+iz$ and also $=\eta+i\zeta$. Then (referring to figure A1) we see that

$$
\begin{aligned}
(\mathbf{N}\cdot\nabla)\int_{S_j}^{S_{j+1}}\gamma(y,z;\eta,\zeta)\,ds' &= \left[-i\,e^{i\alpha_i}\frac{d}{d\hat{z}}\right]\int_{\hat{\zeta}_j}^{\hat{\zeta}_{j+1}}\gamma(\hat{z},\hat{\zeta})\,e^{-i\alpha_j}\,d\hat{\zeta} \\
&= -i\,e^{-i(\alpha_j-\alpha_i)}\times\gamma(\hat{z},\hat{\zeta})\Big|_{\hat{\zeta}_j}^{\hat{\zeta}_{j+1}}
\end{aligned}
\qquad (A1)
$$

where $\hat{\zeta}_j$ is the complex coordinate corresponding to the vertex at S_j and $\hat{\zeta}_{j+1}$ is that corresponding to S_{j+1} . This formula applies to all functions which are harmonic in the interval $[\hat{\zeta}_j,\hat{\zeta}_{j+1}]$.
For instance, if $i\neq j$, we see from (9) that

$$
\begin{aligned}
b_{ij} &= (\mathbf{N}\cdot\nabla)\int_{S_j}^{S_{j+1}} G(\bar{y}_i,\bar{z}_i;\eta(s'),\zeta(s'))\,ds' \\
&= \frac{1}{2\pi}\,\mathrm{Re}\left[\!\!\left[-i\,e^{-i(\alpha_j-\alpha_i)}\left\{\begin{array}{l}\ln\beta_{1i}-\ln\beta_{2i} \\ +2\ \mathrm{p.v.}\int_0^\infty d\nu\,\dfrac{e^{-i\nu\beta_{2i}}}{\nu-k}\end{array}\right\}\right]\!\!\right]_{S_j}^{S_{j+1}} \\
&\quad + i\,\mathrm{Re}\left[\!\!\left[-i\left(e^{-i(\alpha_j-\alpha_i)}\ e^{-ik\beta_{2i}}\right)\right]\!\!\right]_{S_j}^{S_{j+1}}
\end{aligned}
$$

where

$$
\begin{aligned}
\beta_{1i} &= (\bar{y}_i-\eta)+i(\bar{z}_i-\zeta) \\
\beta_{2i} &= (\bar{y}_i-\eta)+i(\bar{z}_i+\zeta)
\end{aligned}
\qquad (A2)
$$

If $i \equiv j$ then the first term of the Green function, $\ln \beta_{ii}$, is not harmonic at the midpoint of the interval $[\hat{\zeta}_i, \hat{\zeta}_{i+1}]$ and the implicit interchange of differentiation and integration in deriving this formula is not valid. For this case, Frank shows that

$$(\mathbf{N}\cdot\nabla)\int_{S_i}^{S_{i+1}} \ln \beta_{ii} = \pi \tag{A3}$$

The expressions for the other terms in (A2) for $i \equiv j$ are correct.

In order to compute the pressure influence functions u_{jk} we have

$$u_{jk} = \int_{S_k}^{S_{k+1}} G(\bar{y}_i, \bar{z}_i; \eta(s'), \zeta(s'))\, ds' \tag{A4}$$

Direct integration by Frank gives the following result

$$u_{jk} = \frac{1}{2\pi} \mathrm{Re}\, e^{-i\alpha_j} \left\{ \beta_{1j} \ln \beta_{1j} - \beta_{1j} - \beta_{2j} \ln \beta_{2j} - \beta_{2j} + \frac{2i}{\nu}\left[\ln \beta_{2j} + \text{p.v.} \int_0^\infty dk\, \frac{e^{-ik\beta_{2j}}}{\nu - k}\right] \right\} \Bigg|_{S_k}^{S_{k+1}}$$

$$+ \frac{i}{\nu} \mathrm{Re}\left\{ e^{-i\alpha_j} e^{-i\nu\beta_{2j}} \right\} \Big|_{S_k}^{S_{k+1}} \tag{A5}$$

When we are dealing with the asymptotic expansion for the Green function (given in (21)). Integration for u_{jk} can be easily evaluated using (A.2) and (A5), inserting the expression for the principal value integral (26).

In dealing with the three dimensional vibration problem we find that the appropriate Green function, $\bar{G}_3$, is not harmonic in the variables β_1 and β_2. We would like, however, to recover a formula for the normal induced velocity comparable to (A1) above. Referring to figure (A1) again, we see that

$$(\mathbf{N}\cdot\nabla) = \sin\alpha_i \frac{\partial}{\partial x} - \cos\alpha_i \frac{\partial}{\partial y}$$

$$\frac{\partial}{\partial x} = \cos\theta \frac{\partial}{\partial r}$$

$$\frac{\partial}{\partial y} = \sin\theta \frac{\partial}{\partial r}$$

Thus $(\mathbf{N}\cdot\nabla) = \sin(\alpha_i - \theta)\frac{\partial}{\partial r}$. Also by inspection, we see that $dr = ds/\cos(\theta-\alpha_j)$, and $ds = -r\,d\theta/\sin(\theta-\alpha_j)$ Whence,

$$(\mathbf{N}\cdot\nabla)\int_{s_j}^{s_{j+1}} \psi(r)\,ds = \sin(\alpha_i-\alpha_j)\,\psi(r)\Big|_{r_j}^{r_{j+1}} + \cos(\alpha_i-\alpha_j)\int_{\theta_j}^{\theta_{j+1}} r\frac{\partial\psi}{\partial r}\,d\theta \qquad (A6)$$

The formula shown in (A6) applies to a real function ψ which is a function of the distance, r, only. Each of the two terms which compose $\bar{G}_3$ (given in (38)) are of this form and are well behaved if $i \neq j$. Once again, if $i \equiv j$, the term $g(\mu|\beta_{1i}|)$ contains a component $\ln|\beta_{1i}|$ which is singular. Since this component is the same as the previous two-dimensional case we get the result shown in (A3) if $i \equiv j$. Otherwise,

$$b_{3,ij} = (\mathbf{N}\cdot\nabla)\int_{s_j}^{s_{j+1}} \bar{G}_3(\bar{y}_i, \bar{z}_i; \eta(s'), \zeta(s'); \mu)\,ds$$

$$= \sin(\alpha-\alpha)\left[g(\mu|\beta_{1i}|) - g(\mu|\beta_{2i}|)\right]\Big|_{s_j}^{s_{j+1}}$$

$$- \cos(\alpha-\alpha)\int_{\theta_j}^{\theta_{j+1}} \left[g'(\mu|\beta_{1i}|) - g'(\mu|\beta_{2i}|)\right]d\theta$$

where $g'(r) = r\frac{\partial g}{\partial r}$. For the pressure influence components, we have

$$u_{3,jk} = \int_{s_k}^{s_{k+1}} \left[g(\mu|\beta_{1j}|) - g(\mu|\beta_{2j}|)\right]ds \qquad (A8)$$

In performing the calculations presented in this paper, the last integral in (A7) and the integral in (A8) were computed numerically using a trapezoidal rule.

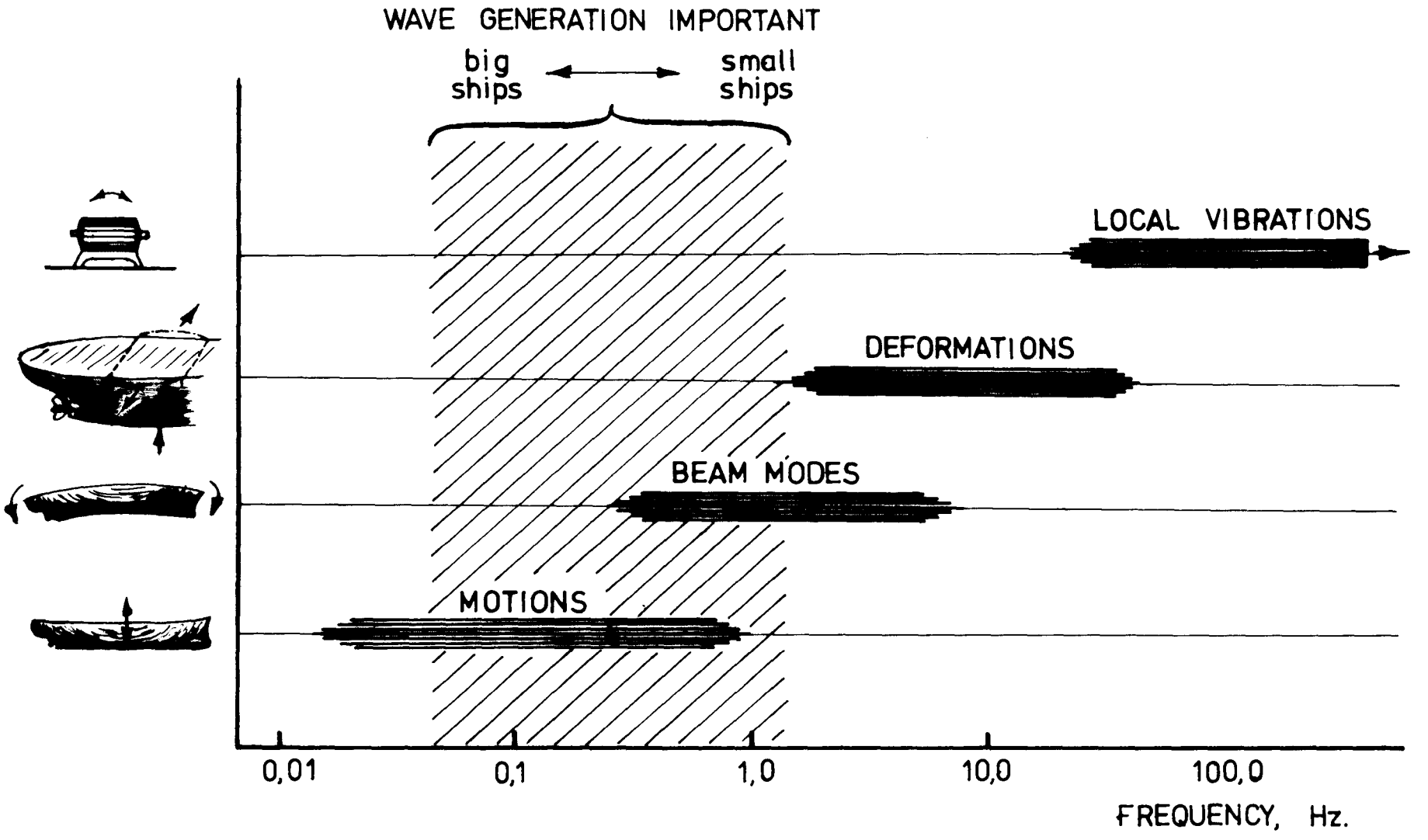

Figure 1. Regimes of Ship Vibrations

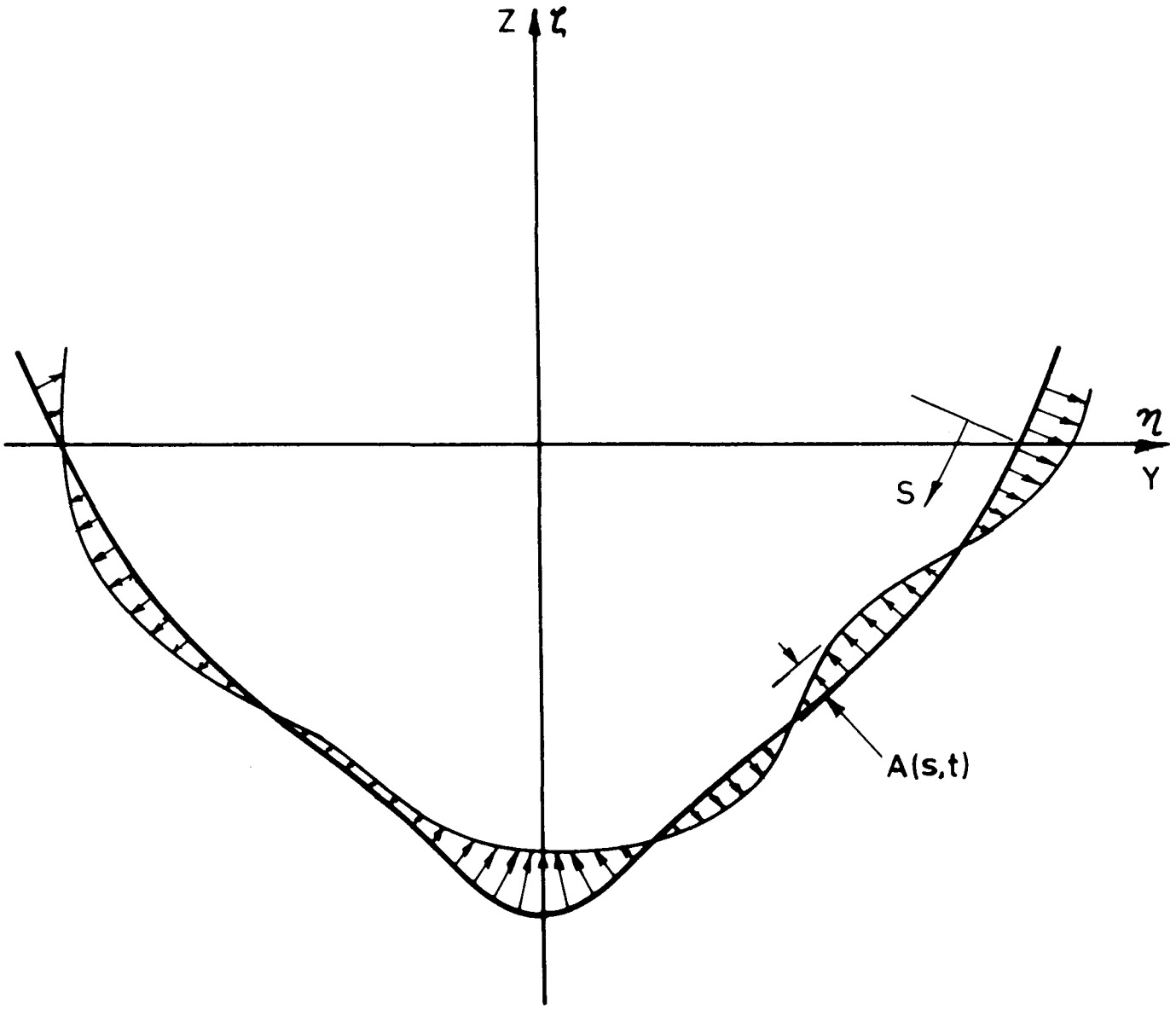

Figure 2. Deformation of an Arbitrary Cross-Section

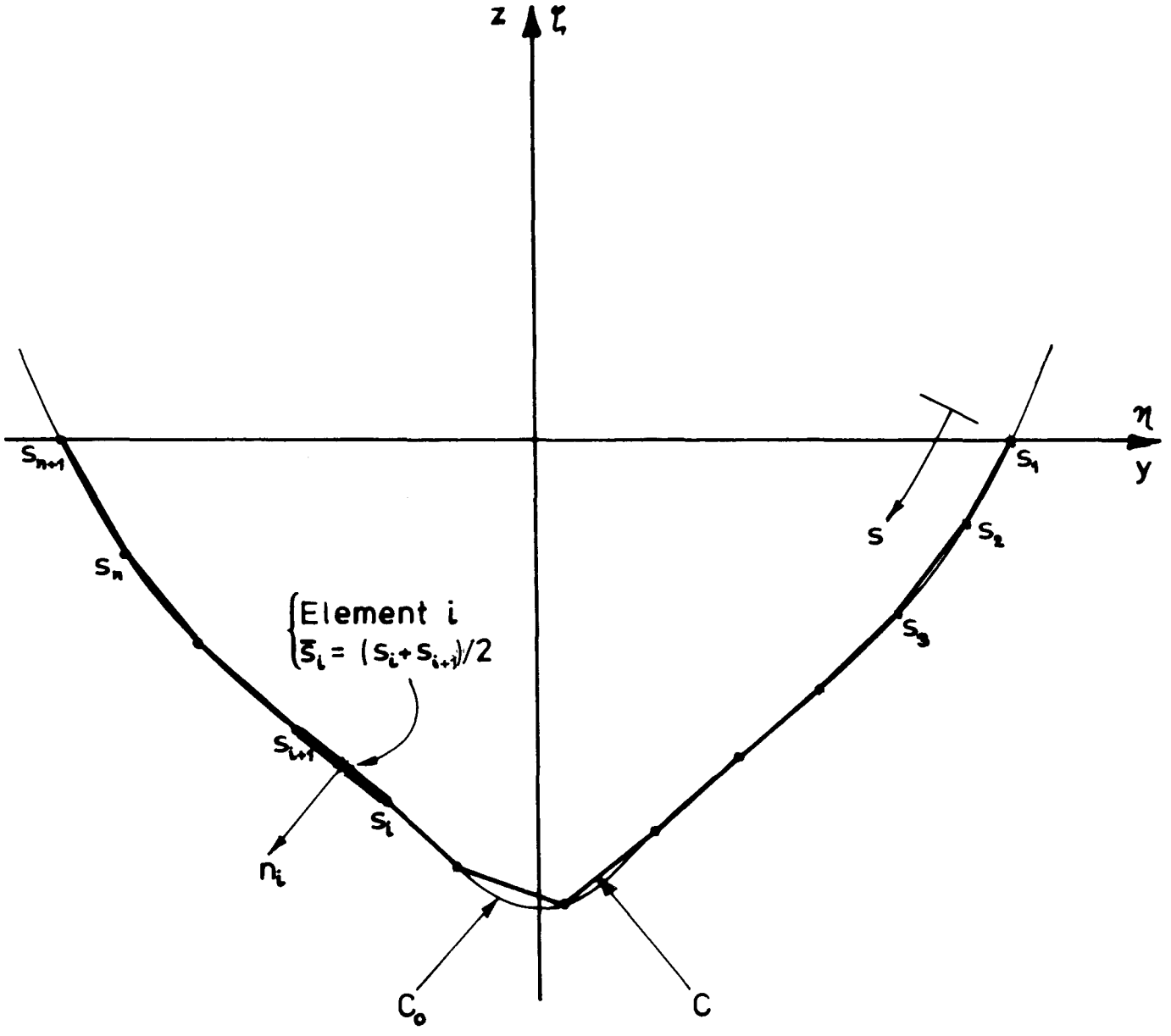

Figure 3. Finite Element Coordinate System

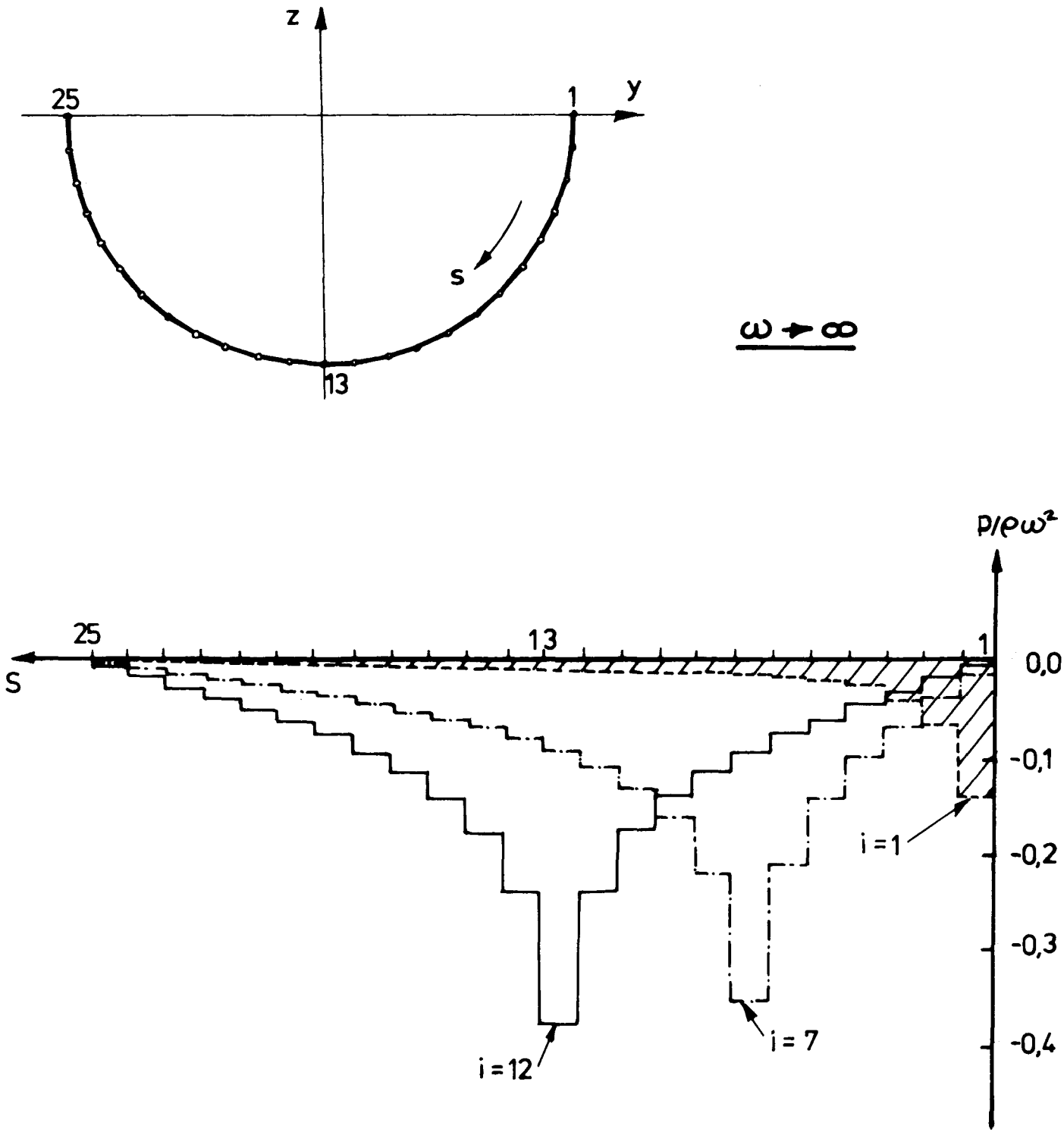

Figure 4. Pressure Influence Functions for a Circular Section

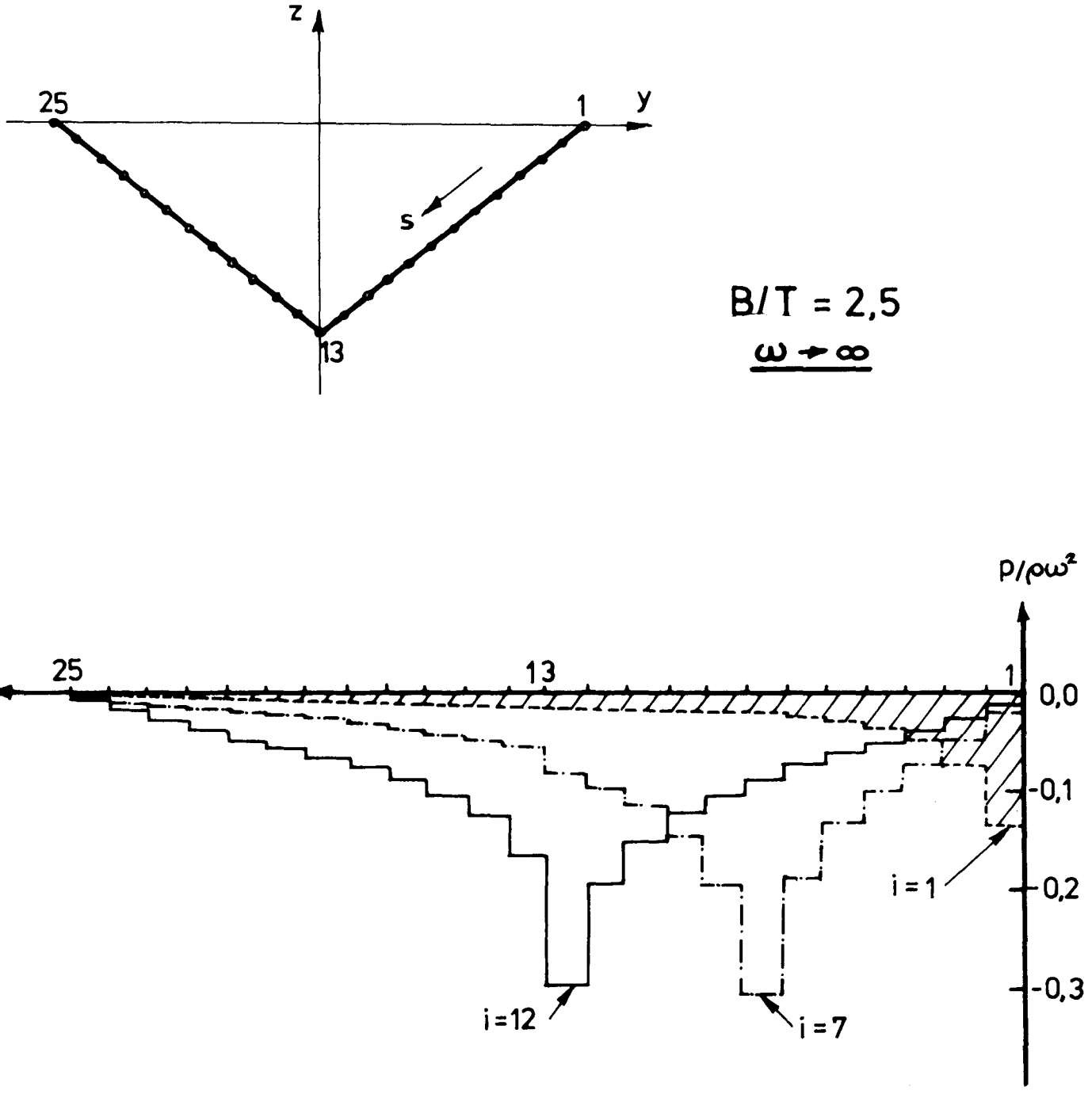

Figure 5. Pressure Influence Functions for a Triangular Section

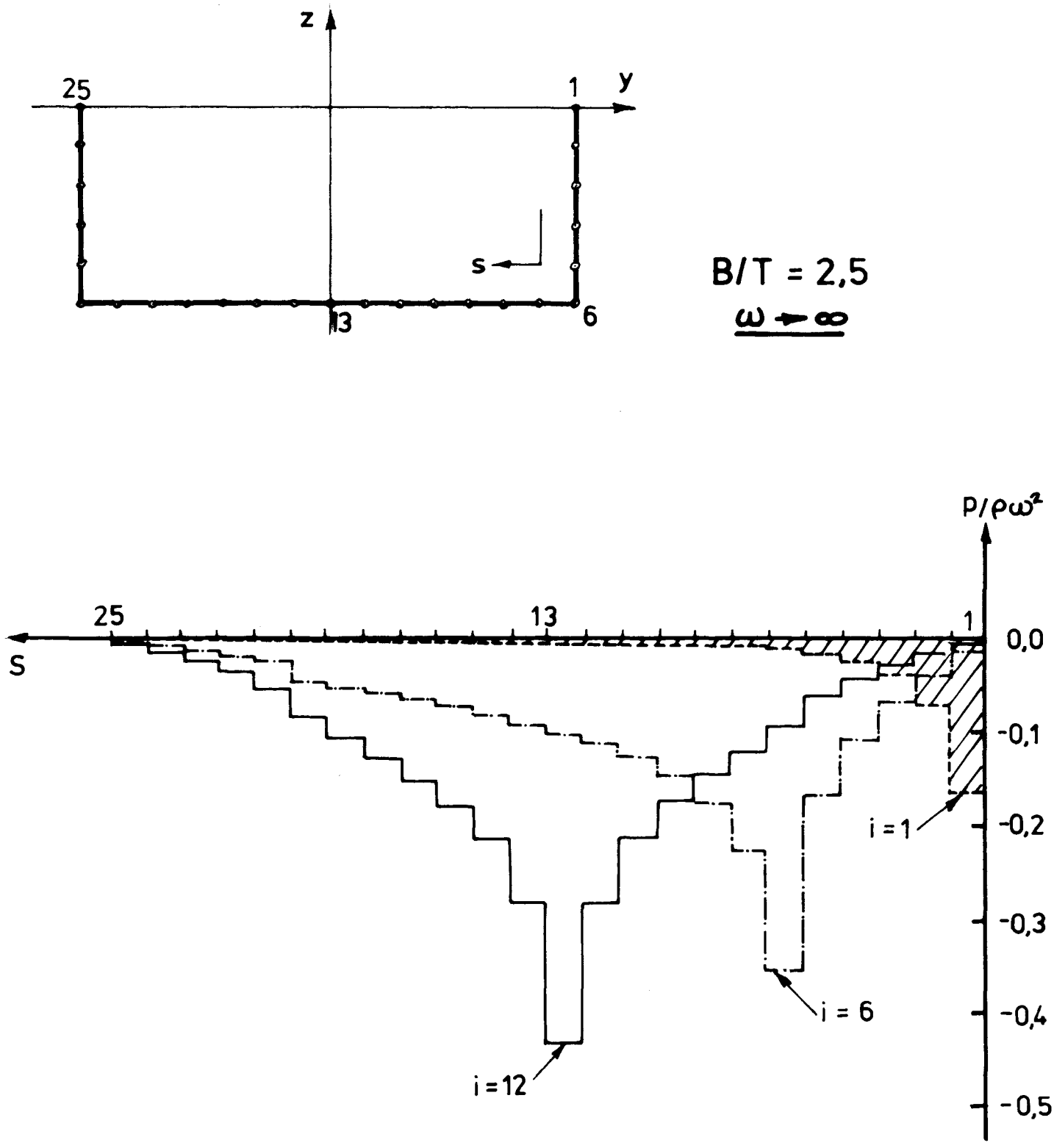

Figure 6. Pressure Influence Functions for a Rectangular Section

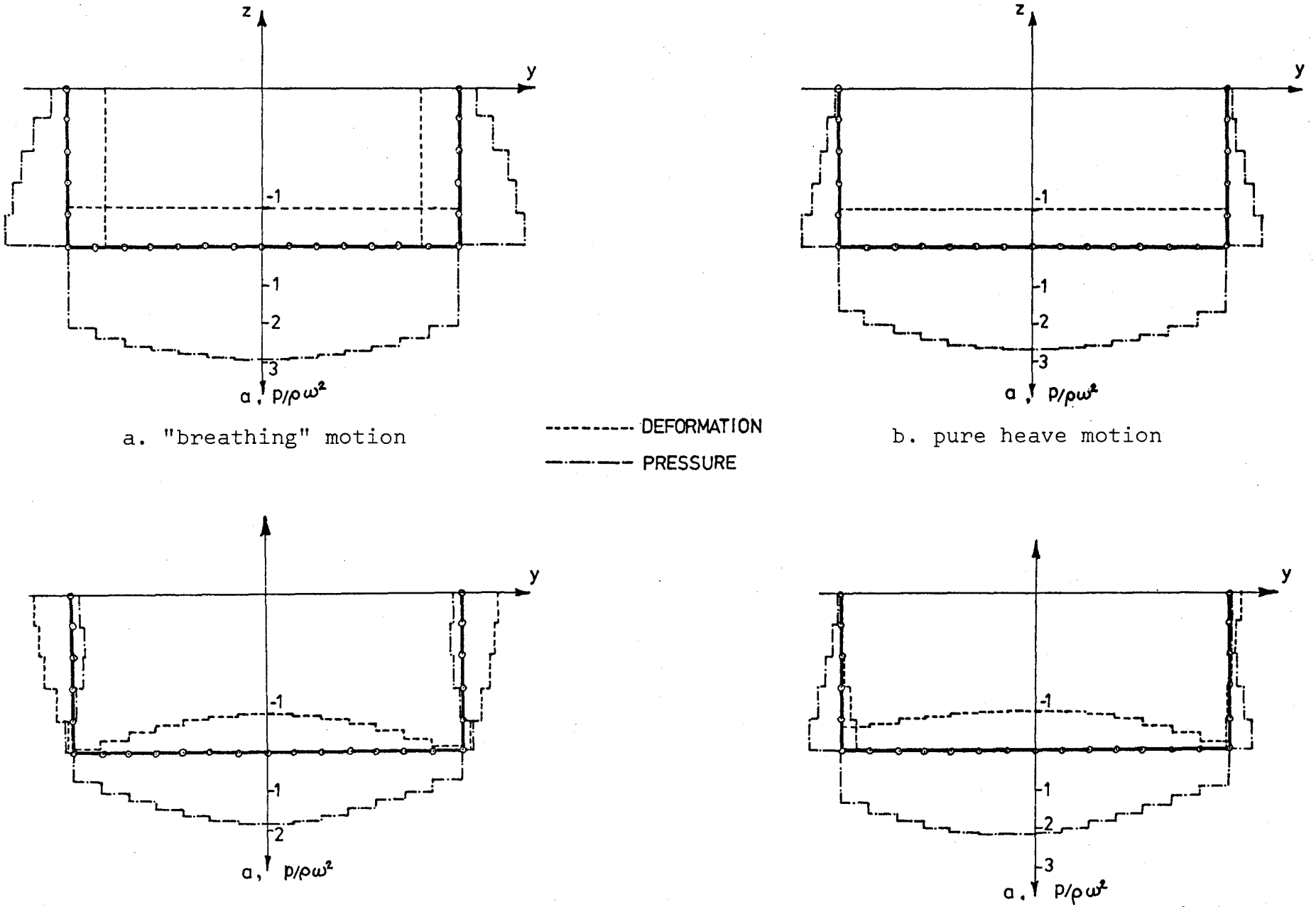

a. "breathing" motion

b. pure heave motion

c. symmetric deformation

d. arbitrary deformation

Figure 7. Hydrodynamic Pressures Resulting from Deformation of a Rectangular Section (B/T = 2.5)

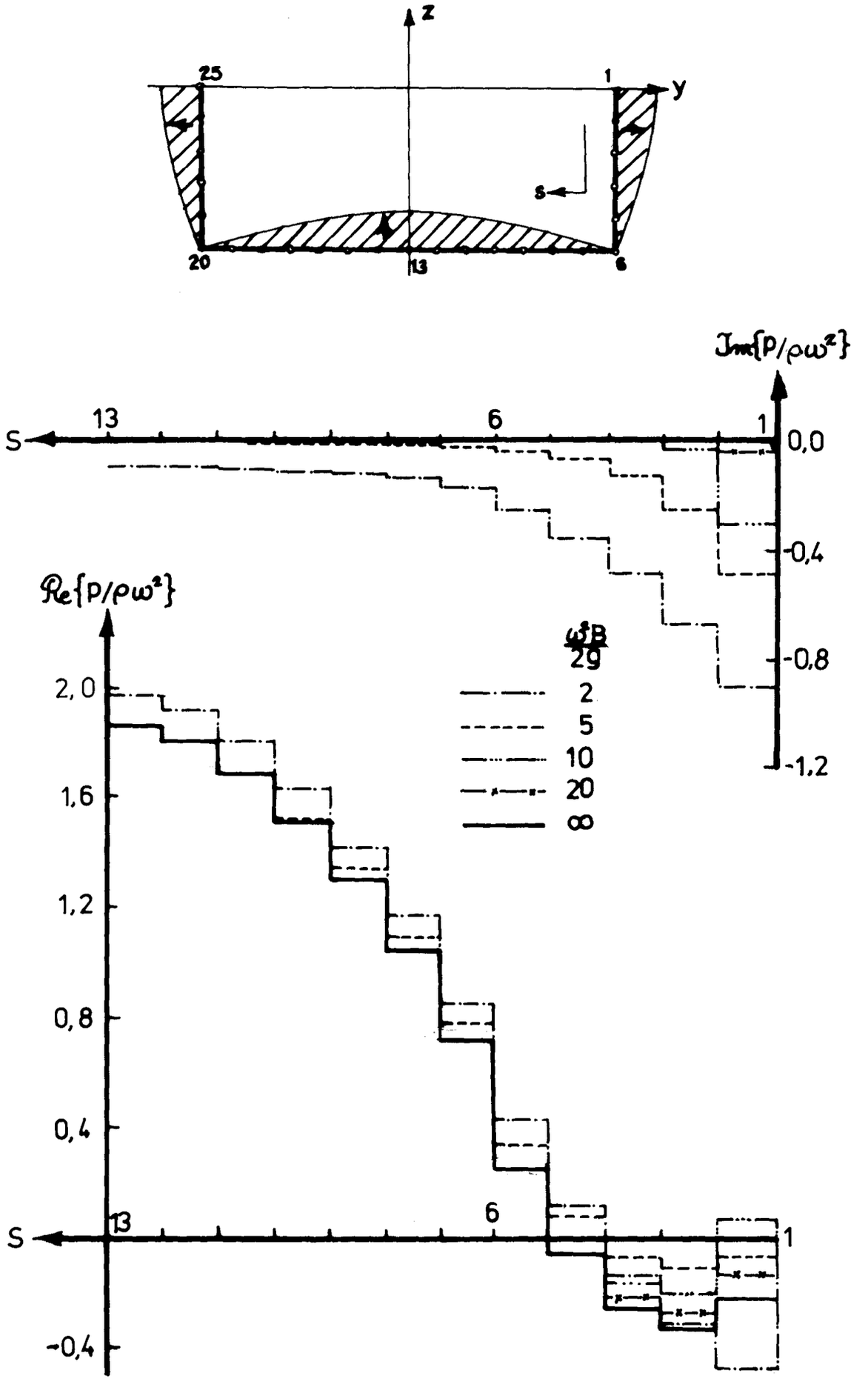

Figure 8. Effect of Finite Frequency on Pressures Induced by Deformation c.

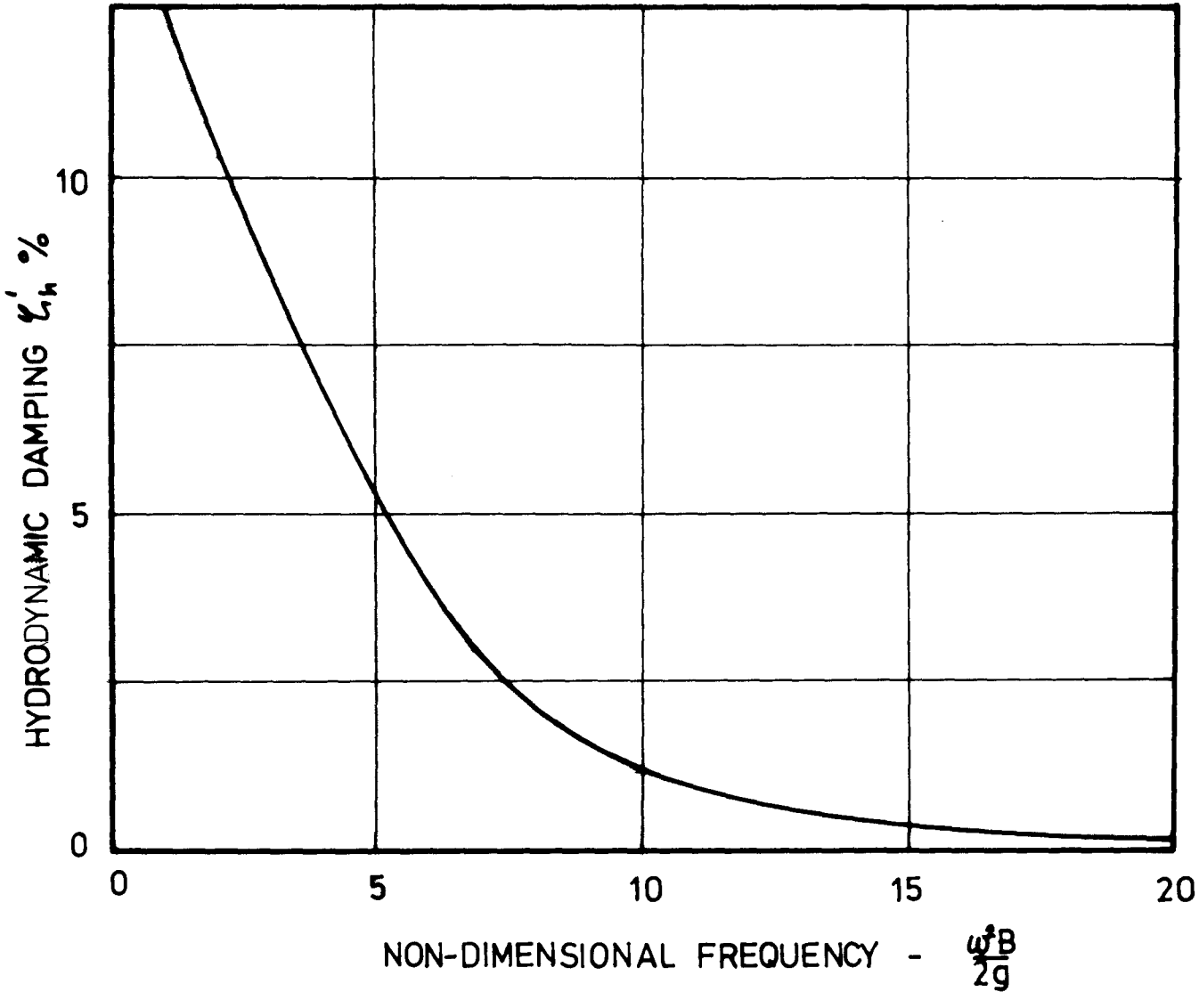

Figure 9. The Effective Hydrodynamic Damping Coefficient as a Function of Frequency for Deformation c.

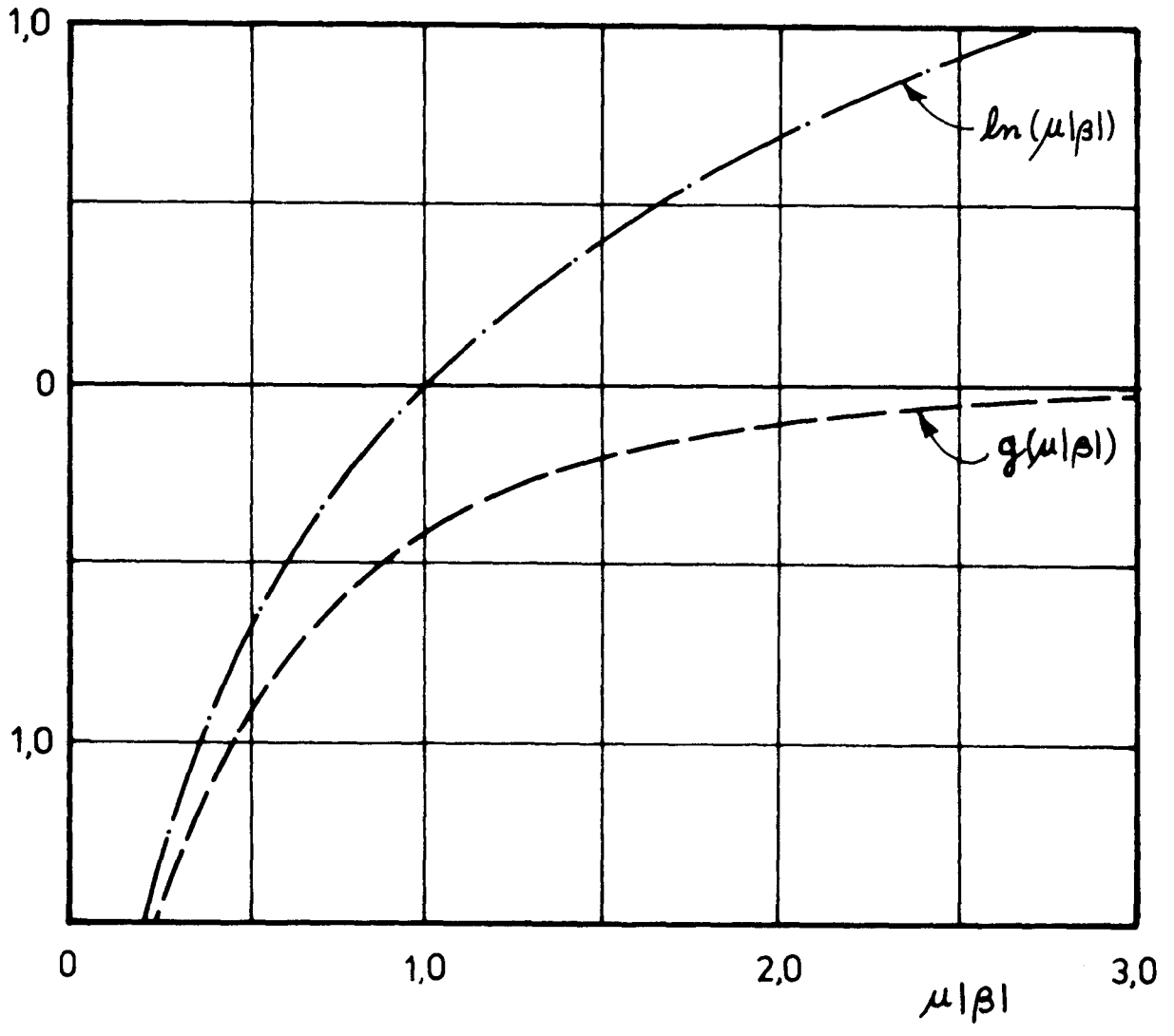

Figure 10. Comparison of Two and Three Dimensional Green Functions

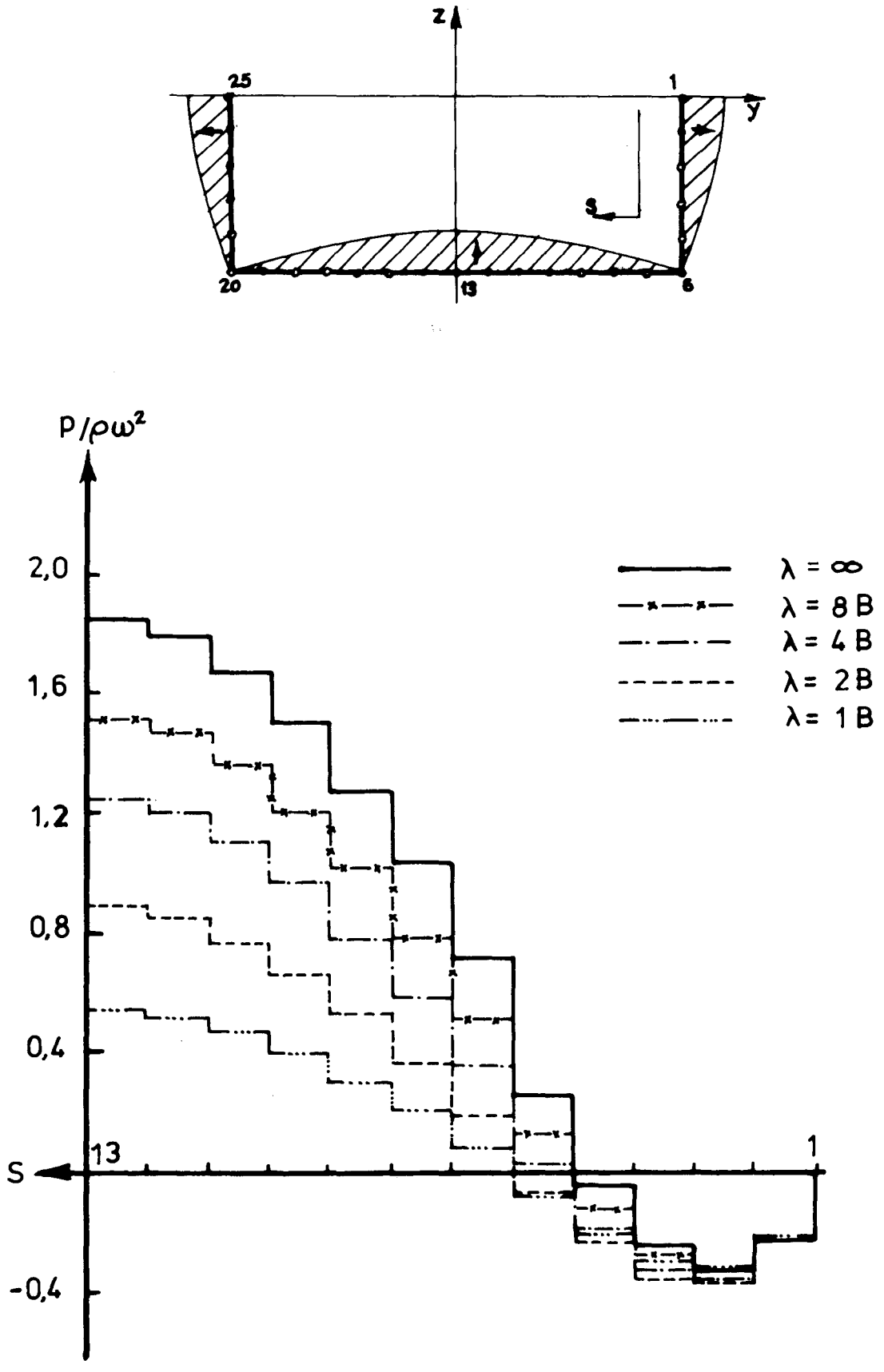

Figure 11. Effect of Lengthwise Variation of Deformation on the Pressure Distribution for Deformation c.

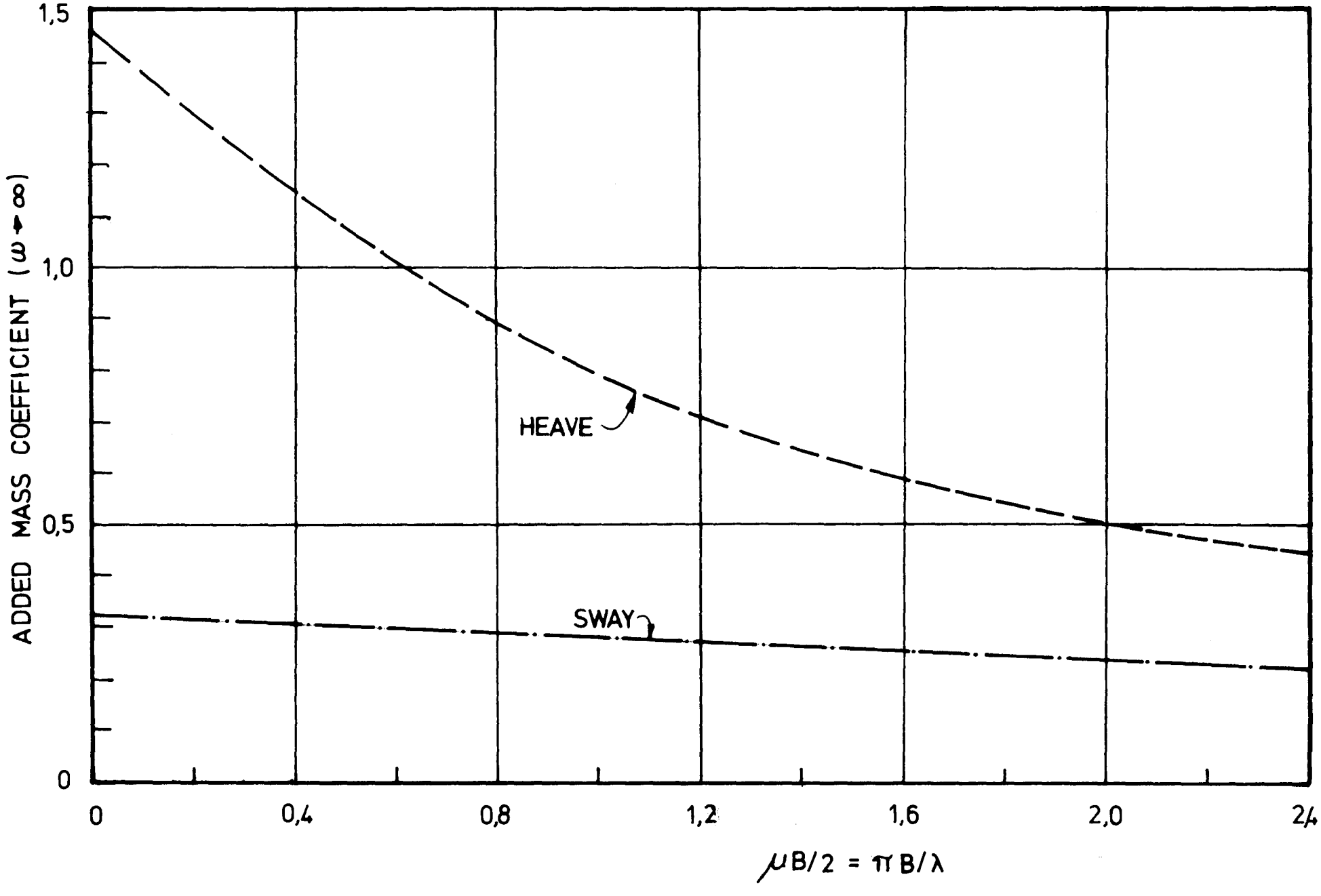

Figure 12. Effect of Longitudinal Variation in Deformation on the Apparent Added Masses

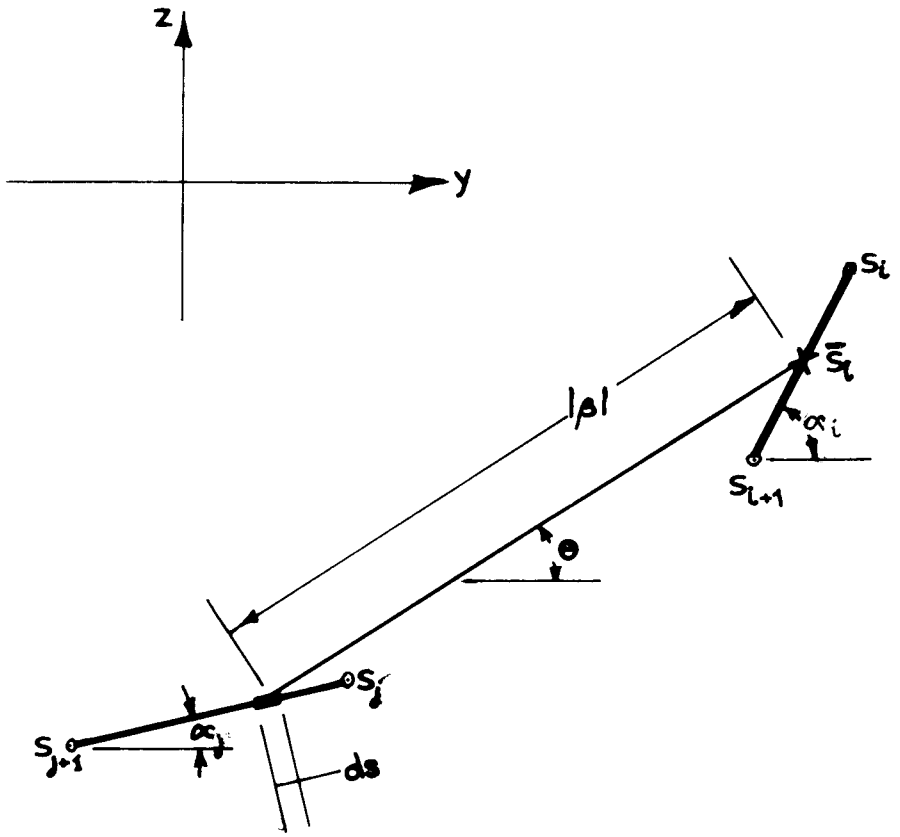

Figure A1. Definitions for Computing the Normal Velocity on Element i Induced by Element j.